XI International Conference on Computational Methods for Coupled Problems in Science and Engineering
COUPLED PROBLEMS 2025
A. Larese, S. Perotto and G. Rozza (Eds)

PARTITIONED APPROACH FOR CONVECTIVE MELTING OF CONSTRAINED, SUBCOOLED SOLIDS

VICTOR VAN RIET[1], WIM BEYNE[1,2] AND JORIS DEGROOTE[1,2]

[1] Department of Electromechanical, Systems and Metal Engineering, Ghent University
Sint-Pietersnieuwstraat 41, 9000 Ghent, Belgium
e-mail: Victor.VanRiet@UGent.be

[2] FlandersMake@UGent – Core lab MIRO, Ghent, 9000, Belgium

Key words: Partitioned method, Solid-liquid phase change, Constrained melting, Front-tracking, Moving-boundary problem

Abstract. This paper extends the partitioned method to constrained melting of subcooled solids. Separate solvers for the solid and liquid phase are coupled by exchanging heat flux and displacement at the interface. The difference between the heat flux coming from the liquid domain and the one entering the solid domain drives the melting. Appropriate mass and energy source terms compensate for the volume increase and decrease in the liquid and solid domains respectively. Two validation problems are solved: the two-phase Stefan problem and a paraffin melting cavity with natural convection. The first simulation shows nearly perfect agreement to the analytical solution. For the two-dimensional melting cavity, the partitioned approach is compared to experimental measurements and fixed-grid numerical simulations, showing very good agreement in terms of interface position, liquid fraction, heat flux, and velocities over time.

1 INTRODUCTION

Melting and solidification play a central role in latent thermal energy storage. These systems store thermal energy by melting a phase change material (PCM), and this heat is later recovered during solidification. As such, they fill an important role in the transition to renewable energy sources by storing excess heat, such as industrial waste heat or electricity converted to heat during periods of high production, for use when demand is high [1]. Therefore, a thorough understanding of the phase change dynamics within these systems is vital to optimise their performance.

Modelling these phenomena poses considerable numerical challenges. The core difficulty lies in the coupling between the solid and liquid phases across a moving interface, which involves sharp changes in material properties and both conduction and convection as heat transfer modes [2]. This has led to the development of various numerical methods to simulate melting and solidification.

Numerical methods for simulating phase change can generally be categorized into fixed-grid (one-domain) and multiple-domain approaches [16]. Fixed-grid methods solve a unified set of governing equations across the entire domain using a stationary mesh. In these methods, phase change effects, such as latent heat release and the absence of motion in the solid phase, must

be incorporated directly into the governing equations. Latent heat is typically included using either enthalpy-based or temperature-based formulations. The enthalpy method, for instance, introduces a volumetric source term in the energy equation to account for latent heat within each computational cell [3]. These approaches do not explicitly track the phase interface; instead, it follows from the computed enthalpy or temperature fields, resulting in a diffuse, non-isothermal transition zone known as the mushy region.

To suppress fluid motion of the solid phase in these fixed-grid methods, a Darcy-like source term is often added to the momentum equation. This term treats the mushy zone as a porous medium, reducing velocity as the liquid fraction approaches zero [3]. When combined with the enthalpy method, this forms the widely used enthalpy-porosity approach, which has been used in numerous studies (e.g., [3, 4]) and is available in commercial solvers like ANSYS Fluent [5]. Alternative techniques for immobilizing the solid phase include artificially increasing viscosity [6] or selectively disabling velocity terms using switching functions [7].

While fixed-grid methods are relatively straightforward to implement, they have limitations. For unconstrained melting, such as close-contact melting in LTES systems, they can overly restrict rigid body motion of the solid phase, exceeding physical constraints [8]. Additionally, these models often rely on fitting parameters, such as the mushy zone constant, which are tuned to match experimental data but reduce the predictive capability across different conditions [9, 10].

In contrast, multiple-domain methods explicitly track the solid-liquid interface, solving separate governing equations in each phase. These include transformed-grid methods [11], deforming-grid approaches [12], and front-capturing techniques [13]. While these methods offer high interface resolution, they are often computationally costly and complex to implement [14, 15]. Their reliance on monolithic solvers also limits flexibility and code reuse.

This work builds on the partitioned front-tracking approach introduced in [16], which aims to retain the advantages of explicit interface tracking while avoiding the complexity of monolithic implementations. In this approach, separate solvers for the solid and liquid domains are coupled by exchanging data at the phase change interface. The present study extends this method to model convective melting of subcooled solids, where a temperature gradient exists in the solid and conduction must be resolved. The interface itself, however, is sharp and remains at the melting temperature.

In the following section, the partitioned method is discussed for a subcooled solid phase. Afterwards, the method is validated with the two-phase Stefan problem and a two-dimensional convective melting problem.

2 NUMERICAL METHODS

Melting problems involve a solid and liquid domain, which are separated by a moving interface. In the liquid region, flow typically occurs, requiring the solution of the mass, momentum, and energy conservation equations. In contrast, the solid region does not allow flow, making the mass and momentum equations trivial inside the solid domain, especially as this work is limited to constrained solids. Only the energy equation needs to be solved, with conduction as the sole heat transfer mechanism.

At the interface, both domains are coupled through a mass and energy balance. The energy balance, also known as the Stefan condition, relates the velocity of the solid-liquid interface to the local difference in heat flux between the solid and liquid domain. Furthermore, a no-slip

boundary condition forces the liquid velocity to be equal to the interface velocity.

In a partitioned approach, the solid and liquid domains are solved independently and the interface conditions are enforced by iteratively exchanging interface data until convergence. As illustrated in Figure 1, heat flux q and interface displacement $\mathbf{u}$ are exchanged for melting problems. The liquid solver computes the heat flux at the interface and passes it to the solid solver, which compares it to the conductive flux within the solid. The resulting difference drives melting and determines the interface displacement via the Stefan condition. This displacement is then returned to the liquid solver and is used to update both computational grids.

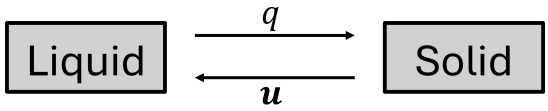

Figure 1: Scalar heat flux q and vectorial interface displacement $\mathbf{u}$ are exchanged to couple the liquid and solid solvers [16].

The primary focus is on the solid solver, as the integration of a subcooled solid within the partitioned approach represents an advancement compared to the previously published work in which the solid was at melting temperature [16].

2.1 Solid domain

The solid solver receives the interface heat flux from the liquid domain and returns the interface displacement as output. In this study, the solid phase may be subcooled, meaning its temperature field lies below the melting temperature, while the interface itself remains fixed at the melting temperature. Consequently, the phase change occurs across an infinitesimally sharp, isothermal interface. The solid is attached to walls and modelled as a constrained rigid body, allowing only conduction as heat transfer mechanism in the subcooled region.

The solid solver is a moving grid arbitrary Lagrangian–Eulerian (ALE) flow solver and has been implemented in ANSYS Fluent 2024R2 for this study. As a result, the convective term only occurs in the energy equation due to the grid velocity $\mathbf{v_g}$, not due to flow velocities. Similarly, the mass equation is only solved to ensure mass conservation on a moving grid.

This section outlines the requirements for the solid solver and its implementation. However, the numerical treatment of the governing equations and the mesh update procedures are handled by the selected solver and do not matter to the coupling algorithm, provided the equations are solved accurately.

Governing equations

Equations 1 and 2 show the integral form of the mass and energy equation solved in a reference frame attached to the solid, with an ALE formulation for the grid movement.

$$\frac{d}{dt}\int_V \rho_S dV + \int_{\partial V} \rho_S \left(-\mathbf{v_g}\right)\cdot \mathbf{n} dA = \int_V S_m dV \tag{1}$$

$$\frac{d}{dt}\int_V \rho_S h dV + \int_{\partial V} \rho_S h \left(-\mathbf{v_g}\right)\cdot \mathbf{n} dA = \int_{\partial V} \lambda_S \nabla T \cdot \mathbf{n} dA + \int_V S_h dV \tag{2}$$

Here, t denotes time, V is the volume of a computational cell, ∂V its boundary surface, $\mathbf{n}$ the normal vector, ρ_S the solid density, T the temperature and λ_S the solid thermal conductivity. The specific enthalpy h can be any function of T the solid solver supports.

S_m and S_h are respectively the mass and energy source terms, which account for the loss of mass and sensible heat in the solid zone during melting. The source terms are only applied to the computational cells adjacent to the interface because only there, melting occurs. Equations 3 and 4 show the discretised form of the source terms.

$$S_m = \frac{-\rho \Delta V_{swept}}{V \Delta t} \tag{3}$$

$$S_h = \frac{-\rho h\left(T_m\right) \Delta V_{swept}}{V \Delta t} \tag{4}$$

In these equations, Δt is the time step size and $h\left(T_m\right)$ is the sensible enthalpy of the solid phase at melting temperature T_m. In case of a constant heat capacity $c_{p,s}$ in the solid, $h\left(T_m\right)$ can be calculated as $c_{p,s} T_m$. ΔV_{swept} is the volume swept by the local cell face on the interface due to its displacement. Each time step, the mass and sensible enthalpy related to swept volume should be removed in each cell containing a moving face on the interface, which explains the negative sign in the source terms. In case of solidification, the solid domain would grow and the source terms would be positive in order to add the necessary mass and enthalpy.

Each cell face is defined by its bounding face nodes. Consequently, the volume swept by a moving cell face over a time step is enclosed by the positions of these nodes at the previous $(n-1)$ and current (n) time steps. In two dimensions, this swept volume reduces to a surface, as illustrated in Figure 2. The moving cell face, being a line segment in 2D, is bounded by two nodes, $\mathbf{r_1}$ and $\mathbf{r_2}$. The resulting swept surface is thus defined by four node coordinates (two from each time step) and its area can be computed using the Shoelace theorem in [16].

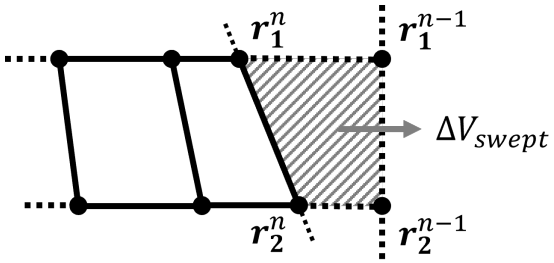

Figure 2: Swept volume is defined by the face nodes $\mathbf{r_1}$ and $\mathbf{r_2}$ at the previous $(n-1)$ and current (n) time step.

The foregoing discussion highlights the important role of grid deformation in both the solid and liquid solvers. The volume change of the computational grid must not only be compensated by appropriate source terms but also introduce convective terms in Equations 1 and 2. These terms account for the motion of the grid itself, represented by the grid velocity $\mathbf{v_g}$ according to the arbitrary Lagrangian–Eulerian (ALE) formulation [17]. Furthermore, the time derivatives in Equations 1 and 2 represent the volume change of the computational cells in time.

The grid velocity depends on the chosen method for grid deformation [17]: spring-based smoothing, Laplace-based smoothing, radial basis functions, linear-elastic behaviour, etc. Computational cells can be added or removed using layering or remeshing techniques. These choices,

however, are made in the separate domain solvers and do not affect the coupling strategy in the partitioned approach. As the focus of the present work is the coupling, the meshing choices will not be elaborated on further in this paper.

Interface conditions

The interface heat flux coming from the liquid domain is used as input for the solid solver. The thermal boundary condition at the interface, however, is not the incoming heat flux, but the interface is fixed at the melting temperature. As such, the heat transfer towards the inside of the solid phase can be calculated from the temperature gradients in the solid. The difference between the incoming heat flux from the liquid and the heat flux going into the solid is used for the melting process itself. This is reflected in the Stefan condition, shown in Equation 5, which is applied to all cell faces on the interface and allows to calculate the local interface velocity from the difference in interfacial heat fluxes.

$$\rho L \mathbf{v_{itf}} = -\lambda_L \nabla T|_L \cdot \mathbf{n} + \lambda_S \nabla T|_S \cdot \mathbf{n} \tag{5}$$

In which $-\lambda_L \nabla T|_L$ and $-\lambda_S \nabla T|_S$ are the interface heat flux from the liquid and solid domain respectively. λ_L and λ_S are respectively the liquid and solid thermal conductivity while $\nabla T|_L$ and $\nabla T|_S$ represent the thermal gradient at the liquid and solid side of the interface. Furthermore, $\mathbf{n}$ is the unit normal on the phase change interface, which means that the interface velocity is assumed normal to the interface, and L is the latent heat of the PCM. Finally, the interface displacement $\mathbf{u}$ during a time step follows from $\mathbf{u} = \mathbf{v_{itf}} \cdot \Delta t$.

At this point, the interface displacement is known at the cell faces, but to update the mesh, the node displacements are required. To obtain interface displacement at the nodes, values defined on the faces are interpolated using a linear *face-to-node* mapping. This procedure must ensure that the interface endpoints remain on the domain boundaries and that local mass conservation is maintained. For details on the iterative *face-to-node* mapping algorithm, the reader is referred to Van Riet et al. [16].

2.2 Liquid domain

The liquid solver takes the nodal interface displacement as input to update its mesh. It then solves the governing equations and returns the heat flux at the interface as output. This section gives a short overview of the liquid solver's functioning. For a more extensive discussion, the reader is referred to [16].

In the current study, the solver is implemented in ANSYS Fluent 2024R2 and the following assumptions are made regarding the liquid domain: incompressible and Newtonian fluid, laminar flow, a two-dimensional geometry and no surface tension at the interface. Furthermore, the PCM is considered a pure, homogeneous and isotropic material which gives rise to a sharp interface with isothermal phase change. The solver allows for temperature-dependent material properties. In particular, a temperature-dependent density can induce natural convection and cause volume changes during phase change.

The conservation equations for mass, momentum and energy are solved in the liquid domain with mass and energy source terms to compensate for the added PCM during melting. The source terms are identical to those in Equations 3 and 4, except for the negative sign, which becomes positive. Instead of removing mass and sensible heat, it is added to the liquid domain

during melting. Furthermore, the swept volume, necessary for the source terms, can be calculated in the same way as in section 2.1, and the volume change can be compensated by the same mesh deformation techniques.

The interface displacement computed in the solid domain is used to update the nodal positions at the interface in both the solid and liquid domains. Although the solid may be subcooled, the interface temperature is assumed constant at the melting temperature T_m. While the interface may initially be below T_m at the onset of melting, this study assumes an initial condition with pre-existing solid and liquid phases separated by an interface at T_m. As a result, the early stages of melting, during which the liquid phase first forms, are not captured within the current partitioned framework and must be handled separately. Additionally, a no-slip boundary condition is applied at the interface, enforcing that the fluid velocity matches the interface velocity $\mathbf{v_{itf}}$ at the moving boundary.

2.3 Coupling strategy and implementation

Figure 3 provides an overview of the coupling strategy used in the partitioned approach described above. In contrast to the earlier method for saturated solids presented by Van Riet et al. [16], the current approach also solves the energy and mass equations within the solid domain. The coupling code itself is solely responsible for the accurate exchange of interface data between the liquid and solid solvers, ensuring that the interface conditions outlined in Section 2 are satisfied. For constrained melting, the exchanged interface variables are heat flux q and interface displacement $\mathbf{u}$.

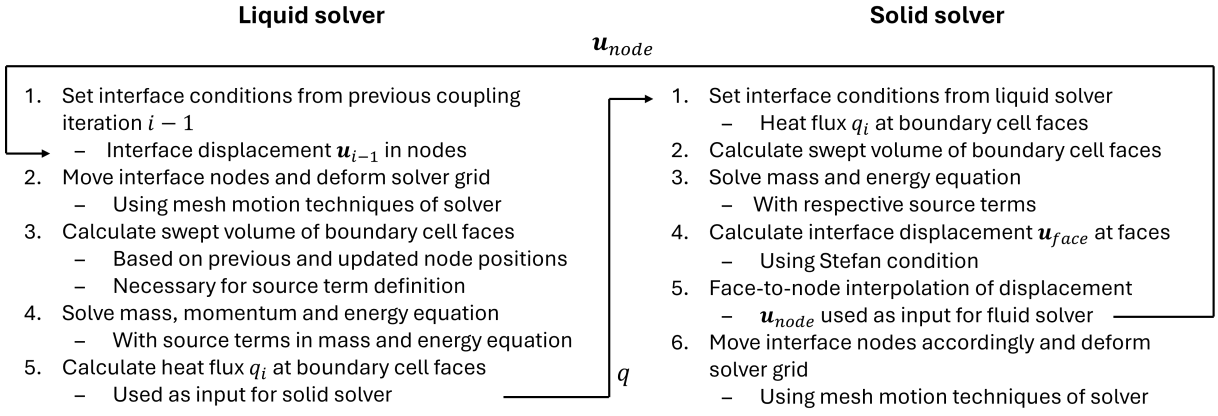

Figure 3: Summary of the coupling strategy.

Each solver is responsible for its own governing equations. The modular design of the coupling code allows integration of different solvers without altering the coupling logic. Only the solver wrapper interacts directly with the solver, handling communication, execution, source terms, and interface conditions. While each solver requires a dedicated wrapper, this is a one-time effort that enables full use of the solver's capabilities, often more advanced than those found in typical research codes for phase change problems.

In this work, ANSYS Fluent is used for both liquid and solid domains, which marks a paradigm shift compared to monolithic front-tracking codes that became overly complex and

case-specific, even for simple melting problem [15]. The partitioned approach avoids these issues by delegating equation solving and grid deformation to robust, validated solvers. The coupling code remains simple, open-source, and modular, with object-oriented design enabling flexibility. Moreover, advanced grid deformation methods, such as spring-based motion and remeshing, are readily available within the solvers.

The solvers can be coupled either explicitly or implicitly, depending on whether interface convergence is enforced. In explicitly coupled simulations, interface data is exchanged once per time step without checking convergence. Implicit coupling, by contrast, involves multiple iterations per time step between the liquid and solid solvers to ensure convergence of the interface conditions within a specified tolerance. Gauss-Seidel iterations sequentially pass the output of one solver to the other. To improve stability in strongly coupled problems, one of the exchanged variables, being the interface displacement $\mathbf{u}$ in this paper, can be modified before being passed on. Common stabilisation techniques include (Aitken) relaxation and quasi-Newton methods [17]. For constrained melting, explicit coupling has proven both stable and accurate, significantly reducing the computational cost of the partitioned approach.

An existing open source coupling code for fluid–structure interaction, CoCoNuT (Coupling Code for Numerical Tools), has been extended to support phase change problems. Its modular architecture enables the integration of solver wrappers for phase change without altering the existing interpolators, predictors, or coupling algorithms. Current implementation limitations include: only 2D problems, only constrained melting (no solidification problems or unconstrained melting yet), isothermal phase change with sharp interfaces and no support for solid topology changes yet. These are implementation-specific and not inherent to the partitioned approach.

3 1D VALIDATION: TWO-PHASE STEFAN PROBLEM

This section compares the analytical solution of the two-phase Stefan problem to the results from the partitioned approach. The two-phase Stefan problem considers conduction-only melting of a subcooled solid phase in a semi-infinite, one-dimensional domain. The solid, which is initially at a uniform temperature T_S below the melting temperature T_m, is heated from a wall $x = 0$ at a temperature $T_L > T_m$. The domain is restricted to a finite length $0 \leq x \leq l$ for the simulation, but a near zero thermal gradient at $x = l$ is ensured throughout the entire duration of the simulation to respect the original problem statement.

The relevant material properties used in this paper are based on the PCM eicosane and are specified in Table 1. Furthermore, the domain length l is chosen at 0.1 m, the heated wall temperature T_L is set to 309.15 K and the right wall is kept at the initial temperature T_S, which is set to 289.15 K.

The analytical solution for the interface position x_{itf} as a function of time t is given in Equation 6 [14]. The variable λ is the unique root of Equation 7. Furthermore, α_L and α_S are the thermal diffusivity of the liquid and solid phase, defined as $k_L/\rho c$ and $k_S/\rho c$ respectively. St_L and St_S are the Stefan numbers of the liquid and solid phase respectively, which are defined as $c\left(T_L - T_m\right)/L$ for the liquid and $c\left(T_m - T_S\right)/L$ for the solid. Lastly, ν is equal to $\sqrt{\alpha_L/\alpha_S}$.

$$x_{itf}\left(t\right) = 2\lambda\sqrt{\alpha_L t} \tag{6}$$

$$\frac{St_L}{\exp\left(\lambda^2\right)\operatorname{erf}\left(\lambda\right)} - \frac{St_S}{\nu\exp\left(\nu^2\lambda^2\right)\operatorname{erfc}\left(\nu\lambda\right)} = \lambda\sqrt{\pi} \tag{7}$$

Table 1: Material properties for the two phase Stefan problem, based on eicosane.

Property	Symbol	Value	Unit
Density	ρ	870	kg/m^3
Specific heat capacity	c	2500.00	J/kgK
Liquid conductivity	k_L	1.5	W/mK
Solid conductivity	k_S	0.024	W/mK
Melting temperature	T_m	299.15	K
Latent heat	L	179000	J/kg

The simulation is initiated halfway through the melting process, at an initial liquid fraction of 0.5. Consequently, both the solid and liquid domains have dimensions of 0.05 m in length and 0.01 m in height, with grids comprising 50 and 10 subdivisions, respectively. This results in square cells with a face length of 0.001 m. Volume changes in both domains are compensated using a diffusion-based smoothing technique. The liquid domain is initialised with a zero velocity field and a temperature distribution according to the Neumann solution for a liquid fraction of 0.5. The top and bottom walls are assigned symmetry boundary conditions.

Both domains are solved using the finite volume solver Fluent 2024R2. The solvers are pressure-based, and central discretisation is applied to both energy and momentum equations due to the absence of non-zero convective terms. A first-order implicit scheme is used for time stepping, with a time step size of 0.1 s. Although the momentum equation is solved, no flow velocities are expected due to the absence of convection in the liquid phase. Finally, the solid and liquid solvers are explicitly coupled.

Figure 4a shows near perfect agreement between the numerical result and analytical solution, which confirms the fundamental coupling strategy and the correct definition of the source terms. As can be seen in Figure 4b, the absolute error never exceeds 10^5 for the liquid fraction. The downwards peak indicates the error switches sign at that point.

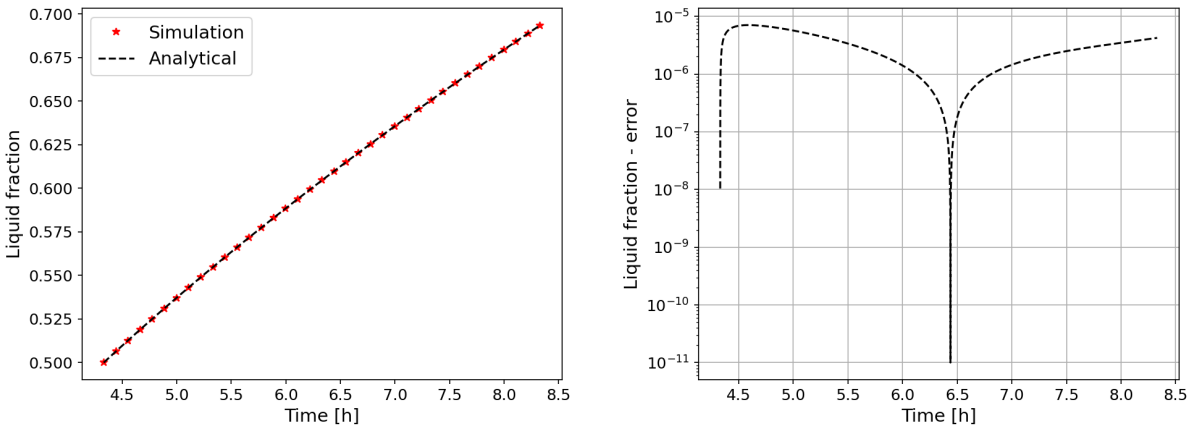

(a) Global liquid fraction as a function of time.

(b) Absolute error of liquid fraction.

Figure 4: Comparison of partitioned simulation to the analytical solution of the Stefan problem.

4 2D VALIDATION: PARAFFIN MELTING

The second validation problem is taken from Faden et al. [18] and considers a melting cavity, which is heated from the left wall. The two-dimensional cavity is square with side walls of 0.04 m. Initially, the PCM is kept at 291.13 K, which is 10 K below melting temperature. At $t = 0$, the PCM is heated from the left wall at a temperature 311.13 K, 10 K above melting temperature, while the right wall is kept at 291.13 K and the top and bottom walls are insulated. The material properties of the PCM are based on octadecane [18] and presented in Table 2. The volume change of the PCM during phase change is compensated by a small outlet located on the left side of the top wall. The outlet is kept at zero gauge pressure and measures 0.0004 m in width. All other walls have a no-slip boundary condition.

Table 2: Material properties of octadecane used as PCM, based on [18].

Property	Symbol	Unit	Solid		Liquid
Density	ρ	kg/m^3	867.914		$979.826 - 0.674 \cdot T$
Heat capacity	c	J/kgK	$-1029 + 9.797 \cdot T$		$3247 - 8.861 \cdot T + 1.821 \cdot 10^{-2} \cdot T^2$
Thermal conductivity	k	W/mK	0.334		$0.246 - 3.121 \cdot 10^{-4} \cdot T$
Dynamic viscosity	μ	kg/ms	$-$		$10^{-3} \cdot \exp\left(-5.353 + 2026.013/T\right)$
Melting temperature	T_m	K	$-$	301.13	$-$
Latent heat	L	J/kg	$-$	236980	$-$

The partitioned simulation is initialised at a global liquid fraction of 0.02, at which point only a narrow liquid gap has formed near the heated wall. Consequently, convective currents are negligible and only conductive heat transfer occurs, resulting in a straight solid-liquid interface. Accordingly, the square cavity is initially split in a rectangular liquid and solid domain with a width of 0.0008 m and 0.0392 m respectively. Furthermore, the temperature field of the liquid and solid domain is initialised with the analytical solution of the two-phase Stefan problem.

Figure 5 shows the grids for both domains. The liquid domain employs an unstructured mesh with two rows of rectangular boundary layer cells at the interface. Domain boundaries are discretized into 800 segments along the vertical walls and 16 along the horizontal, with 8 segments on the top wall designated as the outlet. The solid domain uses a structured mesh with 800 vertical and 400 horizontal subdivisions. Boundary layer cells matching those in the liquid domain are added on the solid side of the interface.

To accommodate volume changes during phase change, the liquid domain uses spring-based smoothing and remeshing, while the solid domain applies diffusion-based smoothing. Boundary layer nodes follow the interface displacement to maintain constant thickness, shifting the interface motion to the outer cells. Both smoothing and remeshing are constrained to a maximum cell skewness of 0.4, using ANSYS Fluent's unified remeshing algorithm [5].

The partitioned simulations are run with two instances of Fluent 2024R2, both using a pressure-based solver. A second-order upwind scheme is applied to convective terms in the energy and momentum equations. Velocity and pressure are coupled via the PISO algorithm, with least-squares cell-based gradients and body-force-weighted pressure interpolation [5]. Time integration uses a second-order implicit scheme with a time step of 0.01 s. The solvers for both domains are explicitly coupled, as stated earlier.

To compare with the partitioned approach, the same problem is solved using the enthalpy-porosity method as implemented in Fluent 2024R2. Once again, a second-order upwind scheme

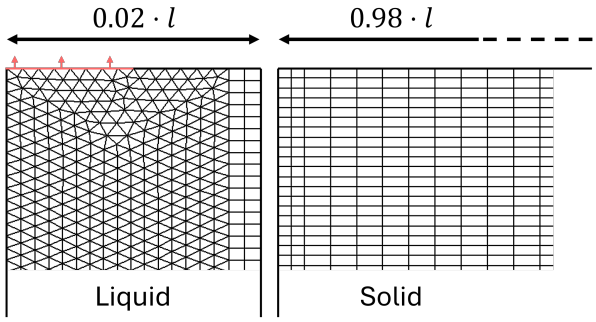

Figure 5: Close up of the liquid and solid computational grids.

is applied to the convective terms with least-squares cell-based gradients, but the velocity and pressure are solved in a coupled fashion and the standard pressure interpolation is used [5]. Based on the grid convergence study in Faden et al. [18], the equations are solved on a structured 200 by 200 grid.

As shown in Figure 6, there is good agreement between the results of the partitioned simulation and those of Faden et al. [18], particularly with their numerical results. Therefore, the small discrepancies between the numerical results and experimental validation are not inherent to the partitioned approach, as they also appear in the results of a fixed-grid simulation. According to Faden et al., the faster melting observed in the numerical results can be attributed to the absence of heat losses compared to the experiment and the two-dimensional simplification of a three-dimensional problem [18].

It is surprising that the Fluent simulation using the enthalpy-porosity method aligns so closely with the experimental results, giving the impression of superior accuracy. This raises the question of why it does not suffer from the same assumptions seen in the partitioned method and Faden et al.'s fixed-grid approach. The explanation lies in a combination of errors: the enthalpy-porosity method fails to fully close the energy balance, resulting in a numerical energy loss, similar to the experimental case, though in this case caused by incomplete convergence of the governing equations at certain time steps during the simulation. As a result, melting occurs more slowly, bringing the results closer to the experimental data. Over the course of the simulation, 176.4 kJ enters the system, while the total enthalpy increases by only 167.7 kJ, a 5% difference. The partitioned simulation is also faster, completing in 12.35 days on the same machine compared to 18.12 days for the monolithic enthalpy-porosity simulation.

The jumps observed in the heat flux results of the partitioned simulation, most clearly visible in Figure 6c, result from a complete remeshing step in both the liquid and solid solvers, in addition to the local remeshing that occurs throughout the simulation. These remeshing steps are necessary to maintain sufficiently small cell faces at the interface, particularly in regions experiencing intense melting.

To assess grid convergence in the partitioned simulation, a coarser grid with twice the cell size, and therefore one-quarter of the total cell count, was also tested. The coarse mesh produced a relative error of 4.44% for the liquid fraction compared to the numerical results of Faden et al., while the fine mesh reduced the relative error to only 0.4%, confirming the mesh convergence.

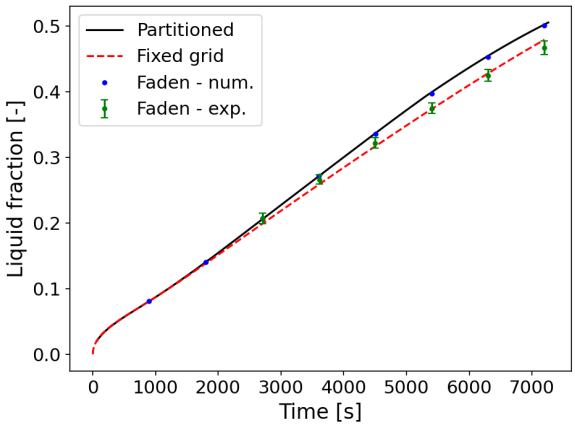

(a) Global liquid fraction as a function of time.

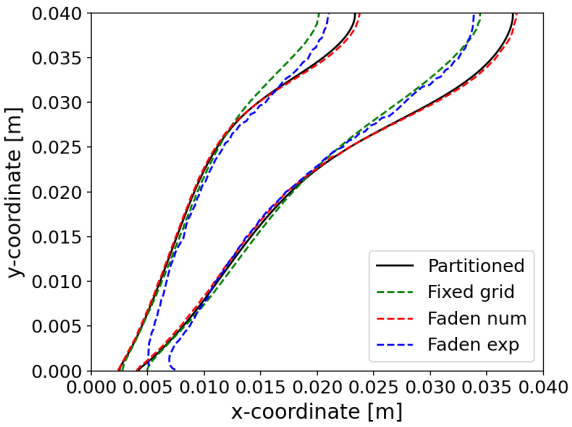

(b) Interface position after 1 and 2 hours.

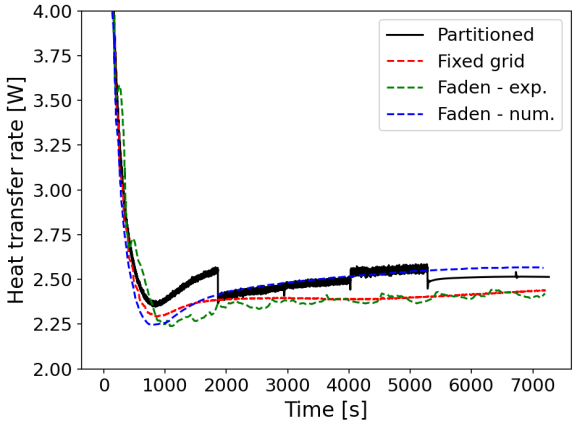

(c) Heat transfer rate at the heated (left) wall.

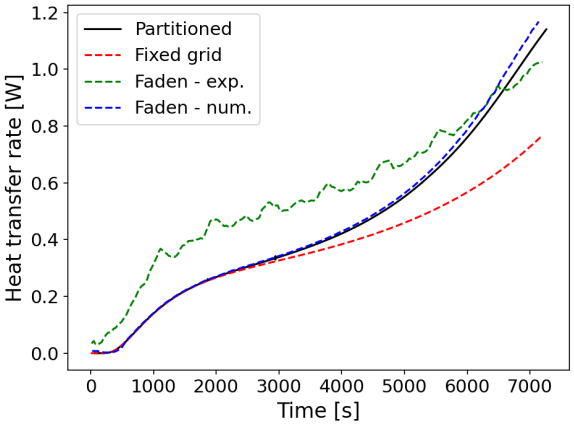

(d) Heat transfer rate at the cooled (right) wall.

Figure 6: Comparison of the partitioned simulation to the results in Faden et al. [18] and simulation results from the enthalpy-porosity method.

5 CONCLUSIONS

This paper expands the partitioned approach for solid-liquid phase change to subcooled solids. In this approach, a separate solver is used for the solid and liquid phase, which are coupled by exchanging heat flux and displacement at the interface. A part of the heat flux coming from the liquid domain now passes into the solid phase; only the difference between both contributes to the melting.

This approach is first validated with the two-phase Stefan problem, a one-dimensional problem with only conductive heat transfer. Near perfect agreement is achieved, validating the coupling strategy. Secondly, the partitioned method is compared to experimental and numerical results for a two-dimensional melting cavity with convection. Very good agreement is reached for liquid fraction, heat flux, and velocities over time, especially with the numerical reference.

The partitioned approach departs from complex monolithic front-tracking codes by using a dedicated flow solver for both phases, allowing robust equation solving and grid handling while keeping the coupling code simple, modular, and open-source. Future development is directed

towards melting of unconstrained solids. In such a case, rigid body motion of the solid should be predicted as well by exchanging pressure and traction forces on the interface.

REFERENCES

[1] Fernández, A. I., Barreneche, C., Miró, L., Brückner, S. and Cabeza, L. F. 19 - Thermal energy storage (TES) systems using heat from waste. in Advances in Thermal Energy Storage Systems (ed. Cabeza, L. F.) 479–492 (Woodhead Publishing, 2015).

[2] Blais, B. and Ilinca, F. Development and validation of a stabilized immersed boundary CFD model for freezing and melting with natural convection. Comput Fluids 172, 564–581 (2018).

[3] Voller, V. R. and Prakash, C. A fixed grid numerical modelling methodology for convection-diffusion mushy region phase-change problems. Int J Heat Mass Transf 30, 1709–1719 (1987).

[4] Hannoun, N., Alexiades, V. and Mai, T. Z. A reference solution for phase change with convection. Int J Numer Methods Fluids 48, 1283–1308 (2005).

[5] ANSYS Inc. Ansys Fluent Theory Guide. (2024).

[6] Kasibhatla, R. R., König-Haagen, A., Rösler, F. and Brüggemann, D. Numerical modelling of melting and settling of an encapsulated PCM using variable viscosity. Heat Mass Transf 53, 1735–1744 (2017).

[7] Ma, Z. and Zhang, Y. Solid velocity correction schemes for a temperature transforming model for convection phase change. Int J Numer Methods Heat Fluid Flow 16, 204–225 (2006).

[8] Shockner, T. et al. Simultaneous close-contact melting on two asymmetric surfaces: Demonstration, modeling and application to thermal storage. Int J Heat Mass Transf 232, 125950 (2024).

[9] Fadl, M. and Eames, P. C. Numerical investigation of the influence of mushy zone parameter Amush on heat transfer characteristics in vertically and horizontally oriented thermal energy storage systems. Appl Therm Eng 151, 90–99 (2019).

[10] Ye, W.-B. and Arıcı, M. Exploring mushy zone constant in enthalpy-porosity methodology for accurate modeling convection-diffusion solid-liquid phase change of calcium chloride hexahydrate. Int Commun Heat Mass Transfer 152, 107294 (2024).

[11] Sparrow, E. M., Patankar, S. v. and Ramadhyani, S. Analysis of Melting in the Presence of Natural Convection in the Melt Region. J Heat Transfer 99, 520–526 (1977).

[12] Mcdaniel, D. J. and Zabaras, N. A least-squares front-tracking finite element method analysis of phase change with natural convection. Int J Numer Methods Eng vol. 37 (1994).

[13] Yoo, J. and Rubinsky, B. A finite element method for the study of solidification processes in the presence of natural convection. Int J Numer Methods Eng 23, 1785–1805 (1986).

[14] Alexiades, V. and Solomon, A. D. Mathematical Modeling of Melting and Freezing Processes. (Taylor and Francis, 1993).

[15] Wang, S., Faghri, A. and Bergman, T. L. A comprehensive numerical model for melting with natural convection. Int J Heat Mass Transf 53, 1986–2000 (2010).

[16] Van Riet, V., Beyne, W. and Degroote J. A partitioned interface-tracking method for convective melting of constrained saturated solids. Int J Heat Mass Transf 254, 127659 (2025).

[17] Degroote, J. Partitioned Simulation of Fluid-Structure Interaction. Archives of Computational Methods in Engineering 2013 20:3 20, 185–238 (2013).

[18] Faden, M., König-Haagen, A. and Brüggemann, D. A combined uncertainty and sensitivity analysis of melting in a cubical cavity, Part A: Model validation. Int J Therm Sci 203, 109144 (2024).